



Status of and materials research at SLS

H.O. Moser^{a,*}, B.D.F. Casse^a, E.P. Chew^a, M. Cholewa^a, C.Z. Diao^a,
S.X.D. Ding^a, J.R. Kong^a, Z.W. Li^a, Miao Hua^a, M.L. Ng^a, B.T. Saw^a,
Sharain bin Mahmood^a, S.V. Vidyaraj^a, O. Wilhelmi^a, J. Wong^a, P. Yang^a,
X.J. Yu^a, X.Y. Gao^b, A.T.S. Wee^b, W.S. Sim^c, D. Lu^d, R.B. Faltermeier^e

^a Singapore Synchrotron Light Source, National University of Singapore (NUS), 5 Research Link, Singapore 117603, Singapore

^b Physics Department, NUS, 2 Science Drive 3, Singapore 117542, Singapore

^c Chemistry Department, NUS, 3 Science Drive 3, Singapore 117543, Singapore

^d Institute of Microelectronics, A*STAR, 11 Science Park Road, Singapore Science Park II, Singapore 117685, Singapore

^e Faltermeier Conservation-Restoration, 8B Keong Saik Road, Singapore 089116, Singapore

Available online 1 August 2005

Abstract

A short overview is given on the status of SLS, its four operational and one forthcoming experimental facilities and their use for material science exemplified by selected work on electromagnetic metamaterials, arrays of nanorods for near-IR photonics, thin films of low dielectric constant materials for semiconductor manufacturing, nanoparticles and art objects.

© 2005 Elsevier B.V. All rights reserved.

PACS: 07.85.Qe; 77.55.+f; 81.05. Mh, Ni, Pj, Qk

Keywords: Synchrotron light source; Microfabrication; Dielectric thin films; Surface analysis; Nanoparticles

1. Status of SLS

SLS is operating a compact 700 MeV electron storage ring that produces synchrotron radiation from two superconducting dipoles which run at a

magnetic flux density of 4.5 T. The characteristic photon energy/wavelength is about 1.5 keV/0.85 nm, respectively. The useful spectral range extends from about 15 keV to the far infrared. Typical beam current after injection exceeds 300 mA. Lifetime ranges between 11 and 17 h depending on beam current.

Four beamlines/experimental facilities are in operation, including the LiMiNT X-ray

* Corresponding author. Tel.: +65 6874 7930; fax: +65 6773 6734.

E-mail address: moser@nus.edu.sg (H.O. Moser).

lithography-based micro/nanotechnology lab with the full LIGA process installed, the PCI white light phase contrast imaging facility, recently upgraded by a tomographic stage, the SINS soft X-ray facility with a spectral range from 50 eV to 1.2 keV featuring photoemission spectroscopy (PES), X-ray absorption fine structure spectroscopy (XAFS), magnetic circular dichroism (XMCD), in situ AFM/STM, a sample preparation chamber and the common characterization equipment and finally, the XDD X-ray diffraction, absorption and fluorescence spectroscopy beamline. The ISMI facility for infrared spectro/microscopy from the visible to the far infrared ($15,000\text{--}10\text{ cm}^{-1}$) is nearing completion, its Fourier transform interferometer and a UHV RAIRS chamber (reflectance absorbance infrared spectroscopy) for studying catalytic surface processes being already available. A schematic layout of SSLS may be found in [1]. Planning in the proposal stage comprises beamlines for X-ray microimaging and microprobe, small angle scattering and the Linac Undulator Light Installation (LIULI) which includes the development of superconducting miniundulators.

2. Materials research

Materials research at SSLS extends into various fields out of which examples from electromagnetic metamaterials, photonics, semiconductor manufacturing and the characterization of nanoparticles and of art work are included in this overview.

Microfabrication of composite materials for electromagnetic applications is pursued with the aim of tailoring the electromagnetic properties of such materials by suitably designing the micropatterns. Fig. 1 shows an array structure of nested split rings and rods made of Au in a plastic matrix of AZ P4620 photoresist. The outer diameter of the larger split ring is $85\text{ }\mu\text{m}$. The design is derived from Pendry et al.'s work [2]. It is expected to become a left-handed material as discussed by Veselago [3] in a narrow frequency range in the THz region. Chips of $2.1 \times 2.1\text{ mm}^2$ area and $14\text{ }\mu\text{m}$ thickness of this material show a resonance at 2.4 THz which agrees well with numerical and analytical predictions of 2.455 and 2.63 THz, respec-

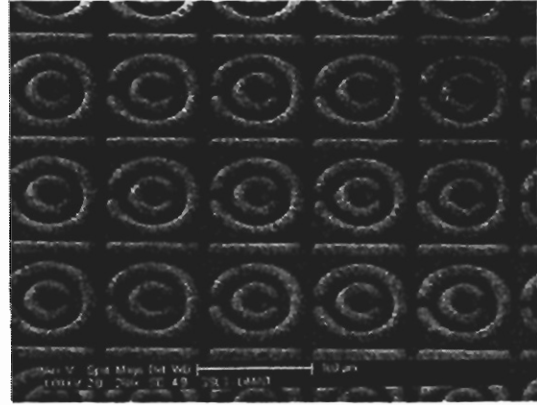


Fig. 1. Array of Au split ring resonators (bright) nested in a plastic matrix consisting of cured AZ P4620 photoresist (dark). The photoresist was patterned by direct laser writing and then used as a template for Au electroplating.

tively. Further experimental work is going on to support the conclusion that this composite material is a metamaterial.

Fig. 2 shows an array of spikes of 200 nm (FWHM) diameter, $2\text{ }\mu\text{m}$ height and $1\text{ }\mu\text{m}$ pitch made by X-ray lithography in PMMA. The respective mask consists of $1\text{ }\mu\text{m}$ high Au pillars on a $1\text{ }\mu\text{m}$ thick Si_3N_4 membrane. Mask fabrication is done in-house at SSLS by electron beam lithography and subsequent electroplating. Besides their interest for chemical and environmental engineering to produce filter membranes with sharply defined holes and almost arbitrary array patterns, such arrays of rods or, complementarily, of holes

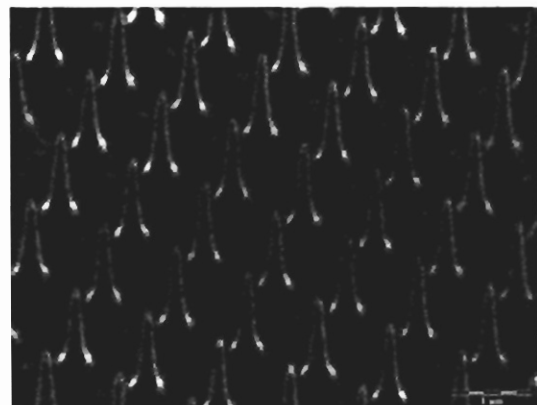


Fig. 2. Array of $2\text{ }\mu\text{m}$ high PMMA needles with diameters 200 nm (FWHM) produced by X-ray lithography.

can serve as dispersing media in demultiplexers for photonics applications in the near infrared or even visible.

The capability to produce very thin layers with a low dielectric constant for insulating wires and electrodes in chips has become an important issue in semiconductor manufacturing. Reflectometry is a method of choice to characterize such functional thin films and multilayers nondestructively after they have undergone various processes such as dry etch and post-etch plasma treatments. As such, it is an important tool for process optimization. Based on the evaluation of rays reflected at all interfaces including the buried ones, reflectometry yields the thickness, refractive index, density, porosity and interface roughness. Fig. 3 shows the specular reflectivity of a Dow Chemical p-SiLK layer after treatment with a $\text{CH}_2\text{F}_2/\text{Ar}$ plasma. Two cut off angles can be seen characterizing the p-SiLK surface and the Si substrate interface. Based on a model that uses Fresnel's formulae for the reflected and refracted rays at any interface, the evaluation of the fringes leads to a thickness of 330 nm and surface roughness of 2.1 nm. More details to describe the usefulness of this powerful method may be found in [4].

Nanoparticles are being widely studied in search of their prospective new or enhanced materials properties. Fig. 4 shows X-ray photoemission spectra (XPS) of $\text{Fe}_{55}\text{Co}_{45}$ nanopowder that has

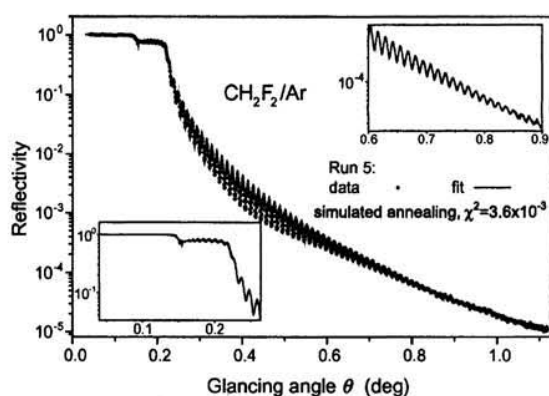


Fig. 3. Specular reflectivity versus glancing angle of a 330 nm thick film of p-SiLK (Dow Chemical) after a $\text{CH}_2\text{F}_2/\text{Ar}$ plasma treatment. The insets are close-ups of the low and high angle region, respectively, and show the quality of both, data and fit.

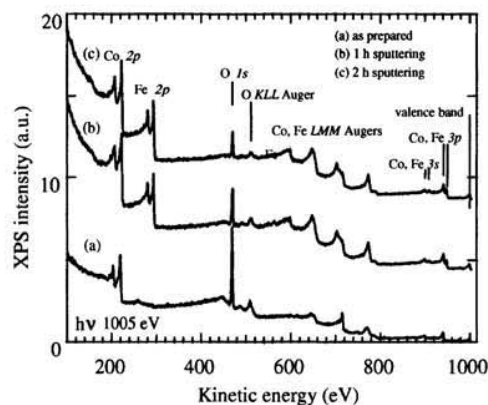


Fig. 4. X-ray photoemission spectra (XPS) of $\text{Fe}_{55}\text{Co}_{45}$ nanopowder as prepared and after sputtering.



Fig. 5. Thai Buddha sculpture (copyright by Faltermeier Conservation-Restoration. With kind permission) at the XDD endstation.

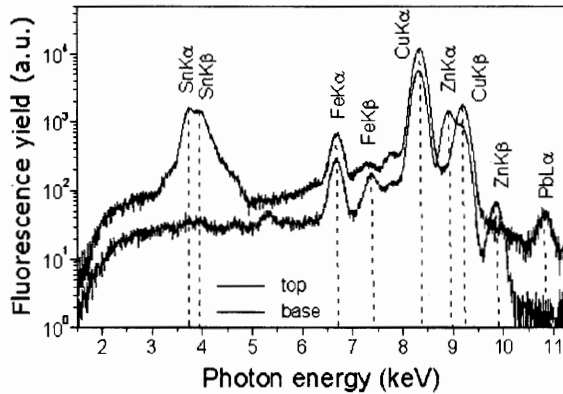


Fig. 6. Fluorescence spectra from the top and the base of the Buddha sculpture showing different Sn and Zn content.

interesting soft magnetic properties. After being produced by ball milling, the powder was characterized by XPS with the result that no iron signal was found while the respective Co peaks were well pronounced. Only when material was gradually removed from the particles' surface by means of sputtering iron peaks showed up and remained stable over 2 h of sputtering. This is explained as evidence of a core-shell structure in which an iron-rich core is surrounded by a cobalt shell. Upon partial removal of the shell the core becomes accessible and the iron peaks show up. Eventually, spectroscopy delivered information about structure.

The final example is about characterization of artwork. Fig. 5 shows a little Thai Buddha bronze sculpture the elemental composition of which was

studied by means of X-ray fluorescence. The spectrum found at the top indicates the presence of Zn such as in brass while the base shows a strong Sn content as in bronze (Fig. 6). Confirmed by X-ray photos (not included here) these findings have shown that the sculpture is pasticcio.

3. Conclusion

The results presented extend into the fields of electromagnetic metamaterials, photonics, semiconductor manufacturing and the characterization of nanoparticles and of artwork. They exemplify the broad range of materials science accessible at SSSL.

Acknowledgments

Work supported by NUS Core Support C-380-003-003-001, A*STAR/MOE RP 3979908M and A*STAR 12 105 0038 grants.

References

- [1] H.O. Moser et al., Nucl. Instr. and Meth. B 199 (2003) 536.
- [2] J.B. Pendry, A.J. Holden, D.J. Robbins, W.J. Stewart, IEEE Trans. Microwave Theory Tech. 47 (1999) 2075.
- [3] V.G. Veselago, Sov. Phys. Uspekhi 10 (1968) 509.
- [4] P. Yang, D. Lu, B. Ramana Murthy, H.O. Moser, Surf. Coat. Technol. 198 (2005) 133.